A Novel Approach to the Study of Solution Structures and Dynamic Behavior of Paclitaxel and Docetaxel Using Fluorine-Containing Analogs as Probes

Iwao Ojima,*,†ꞏ Scott D. Kuduk,† Subrata Chakravarty,† Michèle Ourevitch,‡ and Jean-Pierre Bégué‡

Contribution from the Department of Chemistry, State University of New York at Stony Brook, Stony Brook, New York 11794-3400, and BIOCIS-CNRS, Faculté de Pharmacie, Université Paris-Sud, 5 rue Jean-Baptiste, 92296 Châtenay Malabry, France

Received September 26, 1996⊗

Abstract: Three fluorine-containing paclitaxel and docetaxel analogs, 3′-dephenyl-3′-(4-fluorophenyl)-3′*N*-debenzoyl-3′*N*-(4-fluorobenzoyl)paclitaxel (**3**), 3′-dephenyl-3′-(4-fluorophenyl)docetaxel (**4**), and 2′,10-diacetyl-3′-dephenyl-3′-(4-fluorophenyl)docetaxel (**5**), are prepared and used as probes for the conformational analysis of paclitaxel and docetaxel in aqueous and nonaqueous solvent systems. The dependence of the ^{19}F chemical shifts and the $J_{\text{H2′−H3′}}$ values of these fluorinated analogs is examined through ^{19}F and ^{1}H variable temperature (VT) NMR measurements. The experiments clearly indicate highly dynamic behavior of these molecules and the existence of equilibrium between conformers, especially in protic solvents, i.e., DMSO-d_6/D$_2$O, CH$_3$OD/D$_2$O, and CH$_3$OD, which have not clearly been recognized by the previous studies. The analysis of the VT NMR data in combination with molecular modeling including restrained molecular dynamics (RMD) has identified three key conformers, A, B, and C, in which conformer C possesses rather unusual nearly eclipsed arrangements at the C2′−C3′ bond. Conformers A and C are essentially the same as those identified by X-ray analysis of docetaxel and paclitaxel, respectively. RMD evaluation of conformer C in a simulated aqueous environment shows substantial stabilization of this conformer in protic solvents as compared to the other conformers. The ^{19}F−^{1}H heteronuclear NOE measurements of these fluoro analogs also support the structures of the three conformers. Conformers B and C form a hydrophobic clustering among the 4-fluorophenyl at C-3′, the phenyl at the C-2 benzoate, and the methyl at the C-4 acetate moieties. Since conformer C appears to be the predominant molecular structure at ambient temperature in aqueous solvents, this conformer is likely to be the molecular structure of paclitaxel or docetaxel that is recognized at the tubulin binding site. This study has unambiguously demonstrated the usefulness of these "fluorine probes" for the solution structures and dynamic behavior of complex molecules such as paclitaxel and docetaxel.

Paclitaxel (**1**) and docetaxel (**2**) are extremely important new therapeutic agents approved by the FDA in the treatment of metastatic breast and ovarian cancers.[1−4] Since the first characterization of paclitaxel in 1971,[5] its complex structure, unique mechanism of action,[6−8] and potent antineoplastic activity[9,10] have served as the impetus for intensive studies not only in clinical oncology, but also in the wide range of the biomedical research arena. The mechanism of action of paclitaxel involves stabilization of microtubules by inhibition

of their disassembly process, thereby blocking cell replication. The design of structure- or mechanism-based inhibitors of microtubule disassembly has been hampered by the insufficient information about the three-dimensional tubulin binding site although it may eventually become available on the basis of X-ray analysis or electron crystallography of the tubulin−drug complex[11] and/or photoaffinity labeling and protein sequencing.[12−16] However, the rational design of the second- and third-generation taxoid antitumor agents may well be possible by the combination of the careful analysis of the structural requirements for the strong cytotoxicity of paclitaxel and taxoids, revealed by extensive structure−activity relationship (SAR) studies, and the conformational analysis of these drugs in solution that provides potential models for the biologically relevant conformations for binding to tubulin/microtubules. In

† State University of New York at Stony Brook.

‡ Université Paris-Sud.

⊗ Abstract published in *Advance ACS Abstracts,* May 1, 1997.

(1) Georg, G. I.; Boge, T. C.; Cheruvallath, Z. S.; Clowers, J. S.; Harriman, G. C. B.; Hepperle, M.; Park, H. In *Taxol®: Science and Applications*; Suffness, M., Ed.; CRC Press: New York, 1995; pp 317−375.

(2) *Taxane Anticancer Agents: Basic Science and Current Status*; Georg, G. I., Chen, T. T., Ojima, I., Vyas, D. M., Eds.; American Chemical Society: Washington DC, 1995.

(3) Guénard, D.; Guéritte-Vogelein, F.; Potier, P. *Acc. Chem. Res.* **1993,** *26,* 160−167.

(4) Suffness, M. *Taxol: Science and Applications*; CRC Press: New York, 1995.

(5) Wani, M. C.; Taylor, H. L.; Wall, M. E.; Coggon, P.; McPhail, A. T. *J. Am. Chem. Soc.* **1971,** *93,* 2325−2327.

(6) Shiff, P. B.; Fant, J.; Horwitz, S. B. *Nature* **1979,** *277,* 665−667.

(7) Shiff, P. B.; Horwitz, S. B. *Proc. Natl. Acad. Sci. U.S.A.* **1980,** *77,* 1561.

(8) Vallee, R. B. In *Taxol®: Science and Applications*; Suffness, M., Ed.; CRC Press: New York, 1995; pp 259−274.

(9) Arbuck, S. G.; Blaylock, B. A. In *Taxol®: Science and Applications*; Suffness, M., Ed.; CRC Press: Boca Raton, 1995; pp 379−415.

(10) Rowinsky, E. K.; Onetto, N.; Canetta, R. M.; Arbuck, S. G. *Semin. Oncol.* **1992,** *19,* 646−662.

(11) Nogales, E.; Wolf, S. G.; Khan, I. A.; Ludeña, R. F.; Downing, K. H. *Nature* **1995,** *375,* 424−427.

(12) Rao, S.; Horwitz, S. B.; Ringel, I. *J. Natl. Cancer Inst.* **1992,** *84,* 785−788.

(13) (a) Rao, S.; Krauss, N. E.; Heerding, J. M.; Swindell, C. S.; Ringel, I.; Orr, G. A.; Horwitz, S. B. *J. Biol. Chem.* **1994,** *269,* 3132−3134. (b) Rao, S.; Orr, G. A.; Chaudhary, A. G., Kingston, D. G. I.; Horwitz, S. B. *J. Biol. Chem.* **1995,** *270,* 20235−20238.

(14) Dasgupta, D.; Park, H.; Harriman, G. C. B.; Georg, G. I.; Himes, R. H. *J. Med. Chem.* **1994,** *37,* 2976−2980.

(15) Horwitz, S. B.; Rao, S.; Krauss, N. E.; Heerding, J. M.; Swindell, C. S.; Ringel, I.; Orr, G. A. In *Taxane Anticancer Agents: Basic Science and Current Status;* Georg, G. I., Chen, T. T., Ojima, I., Vyas, D. M., Eds.; ACS Symposium Series 583; American Chemical Society: Washington, DC, 1995; pp 154−161.

(16) Ojima, I.; Duclos, D.; Dormán, G.; Simonot, B.; Prestwich, G. D.; Rao, S.; Lerro, K. A.; Horwitz, S. B. *J. Med. Chem.* **1995,** *38,* 3891−3894.

the course of our study on the development of the second-generation taxoid antitumor agents,[17-23] we have synthesized a series of fluorine-containing taxoids for SAR study.[24] Among these fluorine-containing taxoids, we have found that 3′-dephenyl-3′-(4-fluorophenyl)-3′*N*-debenzoyl-3′*N*-(4-fluorobenzoyl)paclitaxel (**3**), 3′-dephenyl-3′-(4-fluorophenyl)docetaxel (**4**), and 2′,10-diacetyl-3′-dephenyl-3′-(4-fluorophenyl)docetaxel (**5**)-are extremely useful as probes for the investigation into the

1: R = H (paclitaxel)
3: R = F

2: R = R' = R'' = H (docetaxel)
4: R = F, R' = R'' = H
5: R = F, R' = R'' = Ac
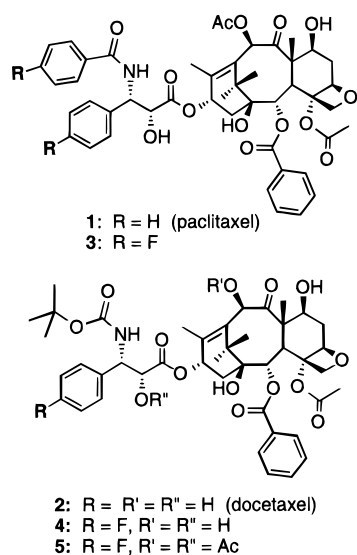
solution structures of paclitaxel and docetaxel, which may well be relevant to bioactive molecular structures, based on ^{19}F and ^{1}H NMR in conjunction with molecular modeling studies. We describe here our study on the solution structures and dynamic behavior of paclitaxel and docetaxel using their fluorine-containing analogs as probes.

The three-dimensional structures of paclitaxel and docetaxel have been studied by NMR in conjunction with molecular modeling[25-33] as well as by X-ray crystallographic analyses.[34,35] These studies identified primarily two conformations, structures **A** and **B**, for paclitaxel (Figure 1) with generally minor variations between different studies.[36]
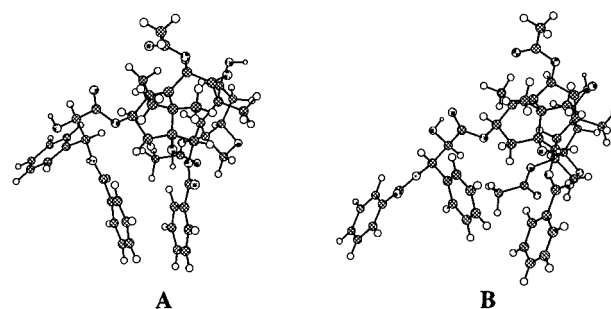

Figure 1. Conformation of paclitaxel based on the X-ray structure of docetaxel and proposed for nonpolar aprotic organic solvents (structure **A**) and the conformation based on the X-ray structure of paclitaxel (structure **B**) proposed for aqueous solvents.

Structure **A** is based on the X-ray crystal structure of docetaxel,[34] replacing the 3′-(*t*-Boc)NH moiety with a 3′-PhCONH group and addition of the 10-acetyl followed by minimization using the Sybyl 6.04 program. The *N*-benzoyl-3-phenylisoserine moiety at C-13 of structure **A** has a gauche conformation with a H2′−C2′−C3′−H3′ torsion angle of ca. 60°. On the basis of molecular modeling simulations (unsupported by NMR studies), there appears to be a hydrophobic clustering among the 3′-PhCONH (Ph), 2-benzoate (Ph), and 4-acetoxy (CH$_3$) moieties. This conformation is believed to be the one commonly observed in aprotic solvents such as CDCl$_3$ and CD$_2$Cl$_2$,[36] and proposed to be the likely bioactive conformation on the basis of unproved assumption that the paclitaxel binding site on microtubules is hydrophobic.[37]

Structure **B** was first recognized by Williams et al. on the basis of conformational analysis of the *N*-benzoyl-3-phenyl-isoserine moiety based on an NMR study and molecular modeling.[26,27] Then, on the basis of 2D NMR experiments (NOESY and ROESY) on paclitaxel and docetaxel in DMSO-d_6/D$_2$O, Vander Velde et al. verified the presence of structure **B** and proposed it as the "hydrophobic collapse conformation"; viz., the Kansas group rationalized this marked conformational change in aqueous media on the basis of the hydrophobic collapse phenomenon[38] rather than intramolecular hydrogen bonding, and implied that this conformation might be the one first recognized by the tubulin binding site.[1,25,39] The *N*-benzoyl-3-phenylisoserine moiety of structure **B** takes on a gauche conformation in which the H2′−C2′−C3′−H3′ torsion angle is ca. 180°, and there is a clear hydrophobic clustering among the 3′-Ph, 2-benzoate (Ph), and 4-acetoxy (CH$_3$) moieties.

(17) Ojima, I.; Slater, J. C.; Michaud, E.; Kuduk, S. D.; Bounaud, P.-Y.; Vrignaud, P.; Bissery, M.-C.; Veith, J.; Pera, P.; Bernacki, R. J. *J. Med. Chem.* **1996**, *39*, in press.

(18) Ojima, I.; Park, Y. H.; Fenoglio, I.; Duclos, O.; Sun, C.-M.; Kuduk, S. D.; Zucco, M.; Appendino, G.; Pera, P.; Veith, J. M.; Bernacki, R. J.; Bissery, M.-C.; Combeau, C.; Vrignaud, P.; Riou, J. F.; Lavelle, F. In *Taxane Anticancer Agents: Basic Science and Current Status;* Georg, G. I., Chen, T. T., Ojima, I., Vyas, D. M., Eds.; ACS Symposium Series 583; American Chemical Society: Washington, DC, 1995; pp 262−275.

(19) Ojima, I.; Park, Y. H.; Sun, C.-M.; Fenoglio, I.; Appendino, G.; Pera, P.; Bernacki, R. J. *J. Med. Chem.* **1994**, *37*, 1408−1410.

(20) Ojima, I.; Fenoglio, I.; Park, Y. H.; Pera, P.; Bernacki, R. J. *Bioorg. Med. Chem. Lett.* **1994**, *4*, 1571−1576.

(21) Ojima, I.; Fenoglio, I.; Park, Y. H.; Sun, C.-M.; Appendino, G.; Pera, P.; Bernacki, R. J. *J. Org. Chem.* **1994**, *59*, 515−517.

(22) Ojima, I.; Duclos, O.; Zucco, M.; Bissery, M.-C.; Combeau, C.; Vrignaud, P.; Riou, J. F.; Lavelle, F. *J. Med. Chem.* **1994**, *37*, 2602−2608.

(23) Ojima, I.; Duclos, O.; Kuduk, S. D.; Sun, C.-M.; Slater, J. C.; Lavelle, F.; Veith, J. M.; Bernacki, R. J. *Bioorg. Med. Chem. Lett.* **1994**, *4*, 2631−2634.

(24) Ojima, I.; Kuduk, S. D.; Slater, J. C.; Gimi, R. H.; Sun, C. M. *Tetrahedron* **1996**, *52*, 209−224.

(25) Vander Velde, D. G.; Georg, G. I.; Grunewald, G. L.; Gunn, C. W.; Mitscher, L. A. *J. Am. Chem. Soc.* **1993**, *115*, 11650−11651.

(26) Williams, H. J.; Scott, A. I.; Dieden, R. A.; Swindell, C. S.; Chirlian, L. E.; Franci, M. M.; Heerding, J. M.; Krauss, N. E. *Can. J. Chem.* **1994**, 252−260.

(27) Williams, H. J.; Scott, A. I.; Dieden, R. A.; Swindell, C. S.; Chirlian, L. E.; Francl, M. M.; Heerding, J. M.; Krauss, N. E. *Tetrahedron* **1993**, *49*, 6545−6560.

(28) Dubois, J.; Guénard, D.; Guéritte-Voegelein, F.; Guedira, N.; Potier, P.; Gillet, B.; Beloeil, J.-C. *Tetrahedron* **1993**, *49*, 6533−6544.

(29) Boge, T. C.; Himes, R. H.; Vander Velde, D. G.; Georg, G. I. *J. Med. Chem.* **1994**, *37*, 3337−3343.

(30) Chmurny, G. N.; Hilton, B. D.; Brobst, S.; Look, S. A.; Witherup, K. M.; Beutler, J. A. *J. Nat. Prod.* **1992**, *54*, 416−423.

(31) Hilton, B. D.; Chmurny, G. N.; Muschik, G. M. *J. Nat. Prod.* **1992**, *55*, 1157−1161.

(32) Baker, J. K. *Spectrosc. Lett.* **1992**, *25*, 31−48.

(33) Falzone, C. J.; Benesi, A. J.; Lecomte, J. T. *Tetrahedron Lett.* **1992**, *33*, 1169−1172.

(34) Guéritte-Voegelein, F.; Mangatal, L.; Guénard, D.; Potier, P.; Guilhem, J.; Cesario, M.; Pascard, C. *Acta Crstallogr.* **1990**, *C46*, 781−784.

(35) Mastropaolo, D.; Camerman, A.; Luo, Y.; Brayer, G. D.; Camerman, N. *Proc. Natl. Acad. Sci. U.S.A.* **1995**, *92*, 6920−6924.
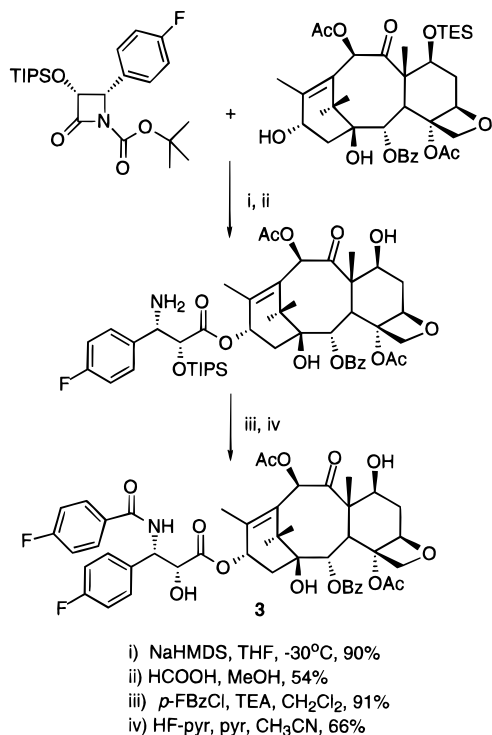
(36) Georg, G. I. For a comprehensive review on the conformational studies on paclitaxel and docetaxel, see ref Georg 1995 **#267**.

(37) Cachau, R. E.; Gussio, R.; Beutler, J. A.; Chmurny, G. N.; Hilton, B. D.; Muschik, G. M.; Erickson, J. W. *Int. J. Supercomput. Appl.* **1994**, *8*, 24−34.

(38) Wiley, R. A.; Rich, D. H. *Med. Res. Rev.* **1993**, *3*, 327−384.

(39) Georg, G. I.; Harriman, G. C. B.; Vander Velde, D. G.; Boge, T. C.; Cheruvallath, Z. S.; Datta, A.; Hepperle, M.; Park, H.; Himes, R. H.; Jayasinghe, L. In *Taxane Anticancer Agents: Basic Science and Current Status*; Georg, G. I., Chen, T. T., Ojima, I., Vyas, D. M., Eds.; American Chemical Society: Washington DC, 1995; pp 217−232.

Scheme 1

i) NaHMDS, THF, -30°C, 90%
ii) HCOOH, MeOH, 54%
iii) *p*-FBzCl, TEA, CH$_2$Cl$_2$, 91%
iv) HF-pyr, pyr, CH$_3$CN, 66%

Scheme 2

i) NaHMDS, THF, -30°C, 98%
ii) HF-pyr, pyr, CH$_3$CN, 90%

Scheme 3

AcCl, DIEA
CH$_2$Cl$_2$, 71%

Recently, this conformation was indeed found in the X-ray crystal structure of paclitaxel obtained by slow evaporation of a dioxane/H$_2$O/xylene solution, in which the H2′−C2′−C3′−H3′ torsion angle is 176°.[35] Even more recently, Gao et al.[40] also found this hydrophobic clustering in the X-ray analysis of 10-deacetyl-7-epipaclitaxel. In the latter case, however, the crystals were obtained from an aprotic solvent, ethyl acetate. Thus, this conformation might be relevant even in a nonaqueous medium.

The conformational analysis of docetaxel led to essentially the same two structures, **A** and **B**, with replacement of the 3′-PhCONH moiety by a 3′-(*t*-Boc)NH group.[36]

In spite of rather extensive NMR studies on the solution structures of paclitaxel and docetaxel mentioned above, no systematic study on the dynamics of these two and other possible bioactive conformations has been reported. It is highly likely that the paclitaxel molecule is dynamic and an averaged structure in the NMR time scale is observed. Accordingly, we decided to look at the temperature dependence of ^{19}F chemical shift(s) of difluoro paclitaxel **3**, fluoro docetaxel **4**, and fluoro diacetyldocetaxel **5**. The use of ^{19}F NMR for a variable temperature (VT) NMR study of the molecule of this complexity is apparently advantageous over the use of ^{1}H NMR because of the wide dispersion of the ^{19}F chemical shifts that allows fast dynamic processes to be frozen out. Also, the sensitivity of ^{19}F NMR is much higher than that of ^{13}C NMR although ^{13}C also offers wide chemical shift dispersion.
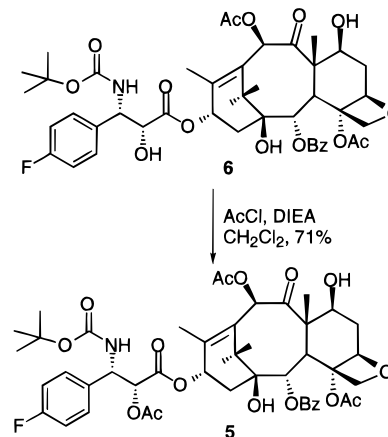
Fluorine probes difluoro paclitaxel **3** and fluoro docetaxel **4** were prepared using the procedures reported previously by us[24] (Schemes 1 and 2), and fluoro diacetyldocetaxel **5** was prepared in a similar manner via acetylation of 3′-dephenyl-3′-(4-fluorophenyl)-10-acetyldocetaxel (**6**)[24] (Scheme 3).

In the cytotoxicity assay, difluoro paclitaxel **3** and fluoro docetaxel **4** showed extremely strong activity (IC$_{50}$ = 0.5−50 nM) comparable to that of paclitaxel; i.e., **3** possesses several times stronger activity while **4** has several times weaker activity than paclitaxel.[41] The observed similar biological activity profile
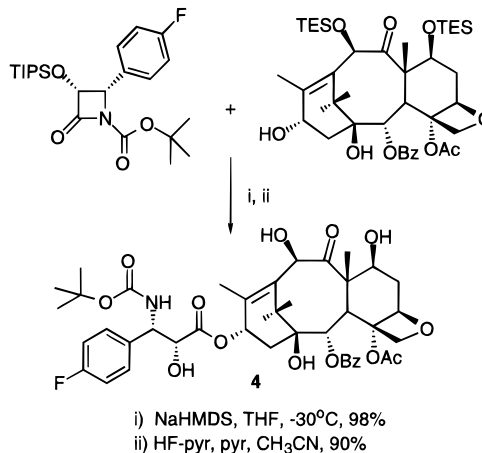
of these fluorine probes should form the basis for the extrapolation of any conformational information to paclitaxel or docetaxel itself.

First, we carried out the VT experiments on the fluorine probes **3** and **4** in CD$_2$Cl$_2$, CD$_3$OD, CD$_3$OD/D$_2$O, and DMSO-d_6/D$_2$O (3:1). The temperature dependence of the ^{19}F chemical shifts of **3** and **4** in these four solvent systems is summarized in Figure 2 (376.3 MHz), and the VT ^{19}F NMR spectra of **3** and **4** in CD$_3$OD (235.2 MHz) are shown in Figure 3.

As Figures 2 and 3 clearly show, the ^{19}F signal (F$_B$) of the 3′-(4-FC$_6$H$_4$) moiety of **3** that appears in a higher field than that of the 4-FC$_6$H$_4$CONH (F$_A$) moiety broadens at ca. 218 K (235.2 MHz) (Figure 3) or at ca. 208 K (376.3 MHz) (Figure 2) in CD$_3$OD. Then, this ^{19}F signal decoalesces into two distinct signals, F$_{B-1}$ (lower field) and F$_{B-2}$ (higher field), with a relative ratio of 3:2. The estimated activation free energy is 39 kJ/mol (9.4 kcal/mol). The VT ^{19}F NMR spectra of **4** show essentially the same phenomenon in CD$_3$OD [E_A = 37.5 kJ/mol (9.0 kcal/mol)] for the 3′-(4-FC$_6$H$_4$) moiety.

This observation unambiguously indicates that two conformers are in equilibrium in a wide temperature range (298−178 K). In sharp contrast with the F$_B$ signal, the F$_A$ signal does not show any significant change except for a small solvent-dependent systematic shift, and no decoalescence is observed. This can be ascribed to either the rapid movement of the 4-FC$_6$H$_4$-CONH moiety even at 183 K or its complete immobility even at ambient temperature. The latter possibility is highly unlikely,

(40) Gao, Q.; Chen, S.-H. *Tetrahedron Lett.* **1996**, *37*, 3425−3428.

(41) The cytotoxicity of difluoro paclitaxel **3** and fluoro docetaxel against human non-small-cell lung cancer (A549) and human ovarian cancer (A121) cell lines are as follows (IC$_{50}$). A549: **3**, 35 nM; **4**, 0.49 nM; paclitaxel, 3.6 nM. A121: **3**, 76 nM; **4**, 1.3 nM; paclitaxel, 6.3 nM.
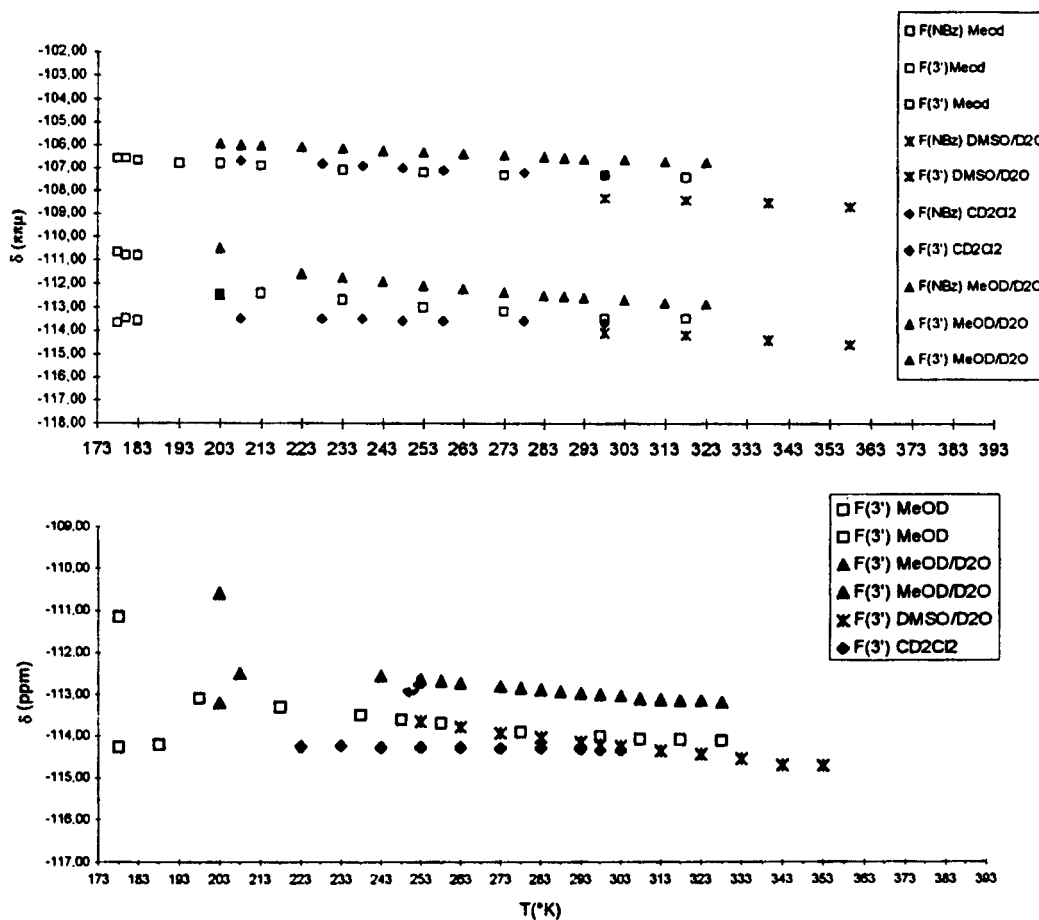
Figure 2. Dependence of ^{19}F chemical shifts of **3** (top) and **4** (bottom) on temperature in different solvents (376.3 MHz).
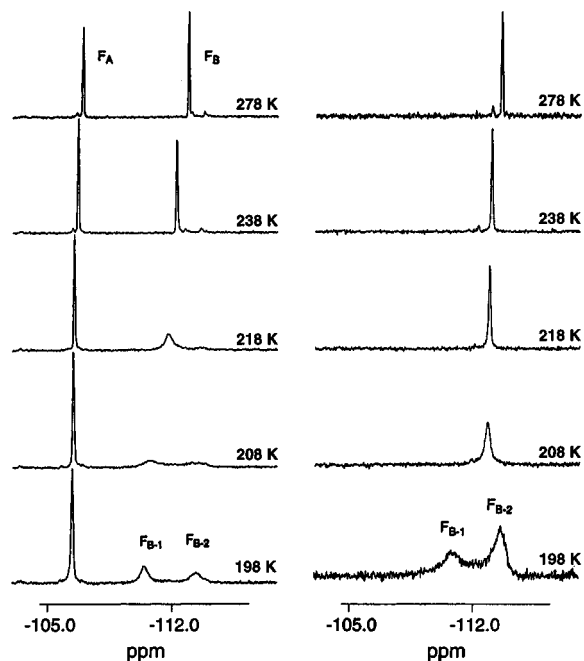

Figure 3. Variable temperature ^{19}F NMR spectra of difluoro paclitaxel **3** (left) and fluoro docetaxel **4** (right) in CD_3OD (235.2 MHz).

and the restrained molecular dynamics (RMD) study (Figure 7) has confirmed the high flexibility of the 4-FC_6H_4CONH moiety. These observations for the F_A and F_B signals strongly suggest the occurrence of hydrophobic clustering including the 3′-(4-FC_6H_4) moiety, and as a result the 4-FC_6H_4CONH moiety is placed in the outside of the hydrophobic cluster.

On the contrary, the chemical shift of the F_B signal does not change at all in CD_2Cl_2. The F_A signal in CD_2Cl_2 shows a small solvent-dependent systematic shift in almost the same manner as that in CD_3OD. No decoalescence is observed even at 173 K. This clearly indicates that there is only one predominant conformer in CD_2Cl_2, which appears to be consistent with the previous NMR studies in this solvent at ambient temperature mentioned above.

In DMSO-d_6/D_2O, the temperature dependence is examined in the range of 253−358 K for **4**, but we observed freezing of this solvent system below 273 K for **3**.[42] The temperature dependence of the F_A and F_B signals is parallel to and follows the same trend as that in CD_3OD. This implies that the equilibrium between different conformers exists in DMSO-d_6/ D_2O as well.

In order to identify the structures of the two conformers observed in CD_3OD and also to confirm the existence of equilibrium between different conformers in DMSO-d_6/D_2O, we looked at the temperature dependence of $J_{H2′−H3′}$ for **3** and **4** in the same set of solvents. Results are shown in Figure 4. As Figure 4 shows, the $J_{H2′−H3′}$ is clearly dependent on temperature for both **3** and **4** in CD_3OD and DMSO-d_6/ D_2O, increasing its value at lower temperatures, whereas the $J_{H2′−H3′}$ in CD_2Cl_2 (ca. 2 Hz) is much less dependent on temperature, slightly increasing at higher temperatures. These observations are consistent with those for the temperature dependence of the ^{19}F chemical shifts for F_B (Figure 2) discussed above.

(42) Vander Velde et al. claimed that NMR study in DMSO/D_2O (3:1) could be performed at −20 °C (see ref 24), but we did not have any luck in keeping the solution from freezing below 0 °C although we were able to obtain clean NMR spectra in the glassy state at −20 °C.
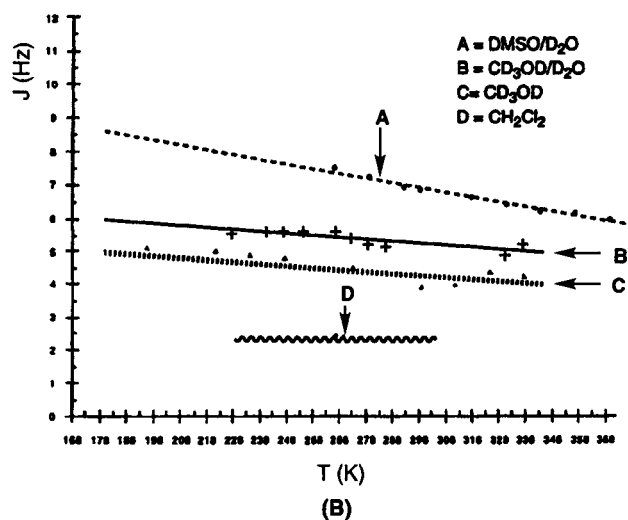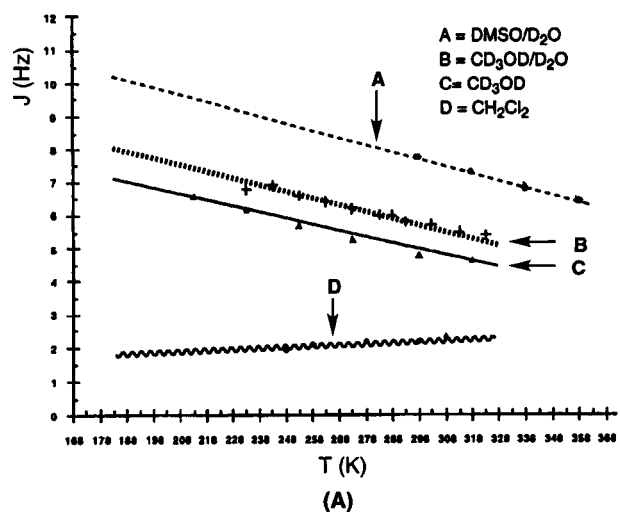
(A)

(B)

Figure 4. Dependence of the coupling constant $J_{H2'-H3'}$ of difluoro paclitaxel **3** (**A**, top) and fluoro docetaxel (B, bottom) on temperature in DMSO/D_2O (3:1) (A), CD_3OD/D_2O (1:1) (B), CD_3OD (C), and CD_2Cl_2 (D) (376.3 MHz).

Since the $J_{H2'-H3'}$ values directly reflect the torsion angle of these two protons, it is possible for us to deduce the conformations of the *N*-benzoyl-3-phenylisoserine moiety at C-13. First, we will discuss the conformational analysis of difluoro paclitaxel **3** based on these NMR data in conjunction with a molecular modeling study.

In CD_2Cl_2, the observed $J_{H2'-H3'}$ value is 2.0 Hz at 258 K, which corresponds to the torsion angle of 54° based on the MM2 calculation (Macromodel 4.0) for the *N*-benzoyl-3-phenyliso-serine moiety (conformer A). This torsion angle (54°) is in good agreement with the one obtained in the X-ray crystal structure of docetaxel.[34]

In CD_3OD, the $J_{H2'-H3'}$ is extrapolated to be 7.2 Hz at 183 K, at which temperature decoalescence takes place (see Figure 2), and this J value should be the average of the J values of the two conformers (3:2 ratio) corresponding to the F_{B-1} and the F_{B-2} signals in Figure 3A. As the slopes A (DMSO-d_6/D_2O), B (CD_3OD/D_2O), and C (CD_3OD) (298−183 K range) in Figure 4A (top) are virtually parallel, it is very reasonable to assume that the same two conformers exist in different ratios in these solvent systems.

In DMSO-d_6/D_2O, the $J_{H2'-H3'}$ value is 7.8 Hz at 298 K that is in good agreement with the reported value by the Kansas group for paclitaxel.[25] *However, as the slope A* in *Figure 4A (top) clearly indicates, this J value should be the average of*
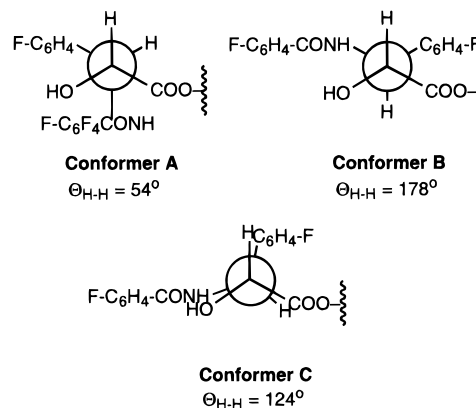

Figure 5. Newman projections of the three conformers of **3**.

the two conformers. The extrapolated J value at 183 K is 10.1 Hz, which corresponds to a H2'−C2'−C3'−H3' torsion angle of 178° based on the MM2 calculation (conformer B). Therefore, this conformer should be exactly the one observed in the X-ray crystal structure of paclitaxel[35] (see structure **B** in Figure 1), and corresponds to the F_{B-2} conformer (higher field signal) since the hydrophobic clustering of the 3'-(4-FC$_6$H$_4$), 2-benzoate (Ph), and 4-acetyl (CH_3) moieties is highly likely to cause a substantial shielding effect. This result is supported by re-strained molecular dynamics (RMD) calculations on conformer B (Figure 7B), which clearly shows a face−edge arrangement of the 3'-(4-FC$_6$H$_4$) and 2-benzoate (Ph) groups in the most stabilized population of conformers. The fluorine on 3'-(4-FC$_6$H$_4$) points toward the center of the 2-benzoate (Ph) ring, and therefore lies in the range of its shielding effect. The $J_{H2'-H3'}$ value of the F_{B-1} conformer is calculated to be 5.2 Hz in a straightforward manner from the J value (10.1 Hz) of the F_{B-2} conformer, the ratio of the F_{B-1} and F_{B-2} conformers (3:2), and the estimated average J value (7.2 Hz) in CD_3OD at 183 K. The J value of 5.2 Hz corresponds to a H2'−C2'−C3'−H3' torsion angle of 124° based on the MM2 calculation; i.e., this is a nearly eclipsed conformation (conformer C). The Newman projections (C2'-C3') of the three conformers of the *N*-phenylisoserine moiety are shown in Figure 5.[43]

The whole structures of conformers A and B (Sybyl 6.04) are virtually the same as the paclitaxel structures **A** and **B** (Figure 1) except for the two fluorine atoms. The Chem 3D representation of conformer C (Sybyl 6.04) is shown in Figure 6. Although this semi-eclipsed conformation at the C2'−C3' bond is obviously unfavorable on the basis of the molecular modeling study of simple *N*-phenylisoserine methyl ester,[27] conformer C has three H-bondings among 2'-OH, 3'-NHCO, and 1'-CO that makes it an apparently favorable conformation as a whole molecule in protic media. *Accordingly, the "fluorine probe" approach has succeeded in finding a new conformer that has never been predicted by the previous molecular modeling studies.*[36]

Strong supporting evidence for this rather uncommon conformation can be found in the solution structure of a water-

(43) For conformers A and C, conceptually there are two possibilities in each case that fit the H2'−C2'−C3'−H3' dihedral angle of 54° or 124°, i.e., −54° instead of +54° and −124° instead of +124°. We looked at these −54° (conformer A') and −124° (conformer C') conformers by RMD in vacuum. Conformer A' showed 1.2 kcal/mol higher energy than conformer A, and no previous NMR studies[25−33] nor X-ray crystal structures of docetaxel[34] and paclitaxel[35] have suggested the importance of this conformer. Conformer C' showed a energy in vacuum RMD very similar to that of conformer C. However, RMD in water revealed 8−10 kcal/mol higher energy than conformer C. Also, the conformation of paclitaxel-7-MPA in D_2O clearly shows a +127° dihedral angle that is, in fact, consistent with our RMD results in water just mentioned above. Consequently, we did not include these two conformers for detailed discussion in this paper.
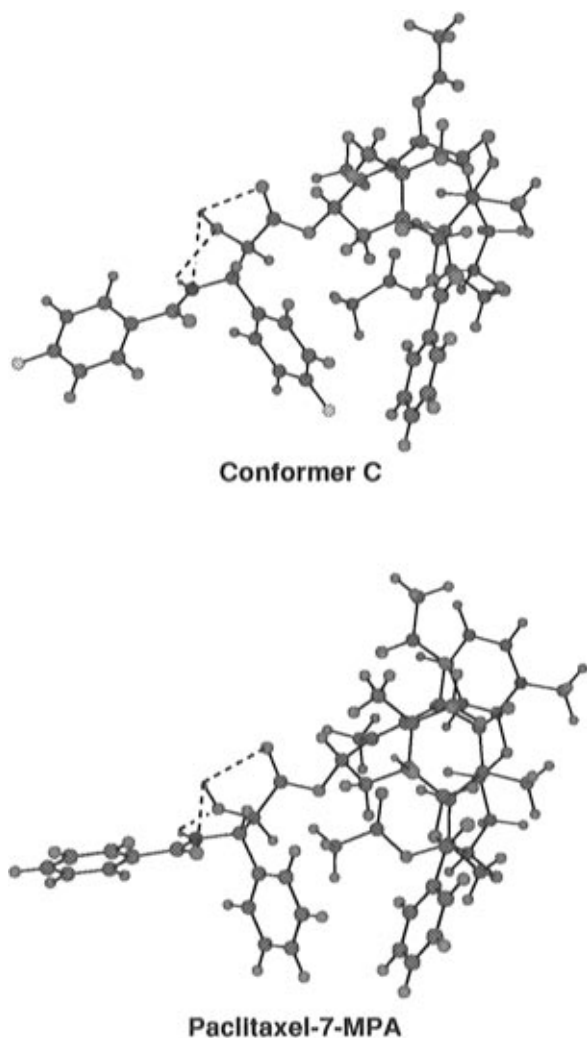
Conformer C

Paclitaxel-7-MPA

Figure 6. Conformer C and the proposed structure of paclitaxel-7-MPA in D_2O.[44]

soluble paclitaxel analog, paclitaxel-7-MPA (MPA = *N*-methylpyridinium acetate), in D_2O reported by Nicolaou and co-workers.[44]   In the proposed structure deduced from NOE constraints in conjunction with molecular dynamics, the H2′–C2′–C3′–H3′ torsion angle of the *N*-phenylisoserine moiety is 127°, which is only a few degrees different from the value for the conformer C (Figure 6).

The major difference between conformer C and the proposed solution structure of paclitaxel-7-MPA is the position of the benzoylamino moieties, i.e., these two are rotamers at the C3′–N and N–CO bonds. The structure of paclitaxel-7-MPA as shown in Figure 6 has three hydrogen bondings as does conformer C. Both structures clearly show similar hydrophobic clustering of the 3′-Ph (or 4-FC_6H_4), 2-benzoate (Ph), and 4-acetoxy (CH_3) groups. However, it is more reasonable to think that the fixation of the movement of the 4-FC_6H_4CONH (or PhCONH) moiety only takes place in the solid state or the frozen state, and this moiety should have high-flexibility in solution at ambient temperature. Accordingly, we carried out high-temperature restrained molecular dynamics (RMD; Sybyl 6.04, Tripos force field) of conformer C, and the overlay of 25 randomly sampled and minimized structures is depicted in Figure 7C. As Figure 7C shows, the 4-FC_6H_4CONH moiety is indeed flexible. *The most remarkable finding in this RMD study is the fact that the molecule shows a good measure of rigidity (except for the 3′-*

(44) Paloma, L. G.; Guy, R. K.; Wrasidlo, W.; Nicolaou, K. C. *Chem. Biol.* **1994**, *2*, 107–112.

acylamino moiety) once the torsion angle of the H2′–C2′–C3′–H3′ is fixed presumably through self-organization by hydrogen bondings and/or hydrophobic clustering. This newly identified conformation might be the molecular structure that is first recognized by the β-tubulin binding site since the contribution of this conformation at around ambient temperature is substantial in protic solvents (see Figure 4).

RMD studies were also carried out for conformers A and B as well (Figure 7A,B). Clearly, conformer A (H2′–C2′–C3′–H3′ constrained to 54°) exhibits a high degree of conformational freedom in the *N*-(4-fluorobenzoyl)-3-(4-fluorophenyl)isoserine moiety as evident by the overlay of 25 structures. Conformer B (H2′–C2′–C3′–H3′ constrained to 178°), however, is much more rigid, exhibiting mostly the hydrophobic clustering structure with some flexibility in the 4-FC_6H_4CONH moiety.

In order to gain some insight into the reason why conformer C becomes the major molecular structure in protic solvents at ambient temperature, we decided to compare the relative energies of the three conformers in a simulated aqueous environment to examine if there is any special stabilization of conformer C as compared to conformers A and B (Figure 8). The energies (enthalpies) in vacuum based on the lowest energy conformer obtained in the RMD simulations (Figure 7) decreases in the order conformer C (83.6 kcal/mol) > conformer A (78.1 kcal/mol) > conformer B (77.8 kcal/mol) (Sybyl 6.04, Tripos force field). This relative order of energies was supported by RMD simulations in vacuum using the Discover 95.0 program (MSI-Biosym, CVFF force field). In comparison, the RMD at ambient temperature in a simulated aqueous environment starting from the lowest energy structure obtained from the RMD studies for each conformer mentioned above indicates the following order in energy: conformer A/nH$_2$O ≥ conformer C/nH$_2$O > conformer B/nH$_2$O.[45–48] Accordingly, the RMD study in an aqueous environment clearly indicates a strong contribution of solvation energy to the stabilization of conformer C *vis-à-vis* conformer A. While the difference in energy between the two conformers in vacuum is appreciable (~ 5 kcal/mol), this difference is completely overcome in aqueous solution where conformer C becomes slightly more stabilized than conformer A. It should be noted that the solvation stabilization term for conformer C is estimated to be about 10 kcal/mol more than those of conformers A and B.

Although this RMD study has revealed strong solvation effects for conformer C, in particular, which can offset, to a certain extent, the destabilization caused by the near-eclipsed

(45) Anderson, A. G.; Hermans, J. *Proteins* **1988**, *3*, 262–265.

(46) Gilson, M. K.; Honig, B. *Proteins* **1988**, *4*, 7–18.

(47) Biosym Technologies, I. *Discover User Guide, Versions 95.0*; 1994.

(48) The energies for each conformer in an aqueous environment (9 Å layer of discrete water molecules) were calculated on the basis of average minimized energy of 25 frames collected at 1 ps intervals during the restrained molecular dynamics sequence (Discover 95.0, CVFF force field, Biosym Technologies/Molecular Simulations Inc.). The average total energies, incorporating a solvation term, calculated for each conformer were the following: conformer A (184.8 ± 3.6 kcal/mol), conformer B (179.8 ± 3.6 kcal/mol), and conformer C (183.9 ± 2.4 kcal/mol). The average solvation energies (calculated as the summation of intermolecular van der Waals and Coulombic interactions) for each conformer were the following: conformer A (−82.6 ± 6.1 kcal/mol), conformer B (−82.6 ± 4.4 kcal/mol), and conformer C (−93.1 ± 4.1 kcal/mol). It should be noted that the numerical values of the total energies depend on the force field used and, as such, are meaningful only for the comparison of relative energies of conformers. It is assumed that the above calculation provides an average energy for the different conformers possible at ambient temperature for each constrained dihedral. However, different factors such as the orientation of water molecules in any particular frame may influence the energy terms without actually being associated with the actual conformational and solvation energies. This study must therefore be considered an approximation only. See the Experimental Section for further details.
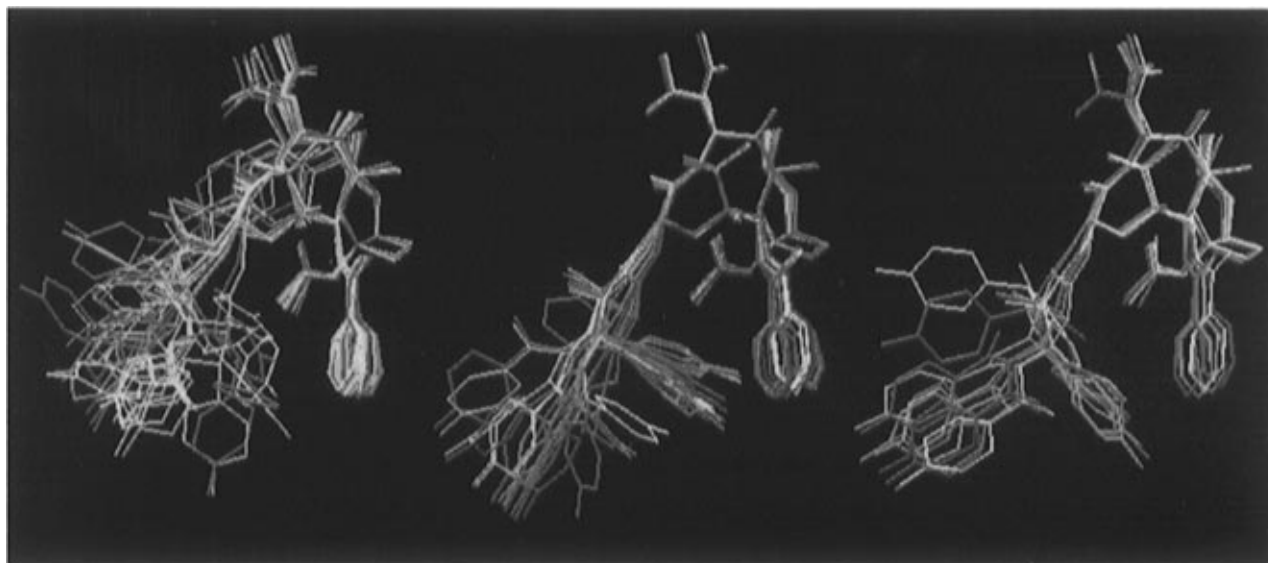
Figure 7. RMD in vacuum for conformers A (left), B (middle), and C (right).
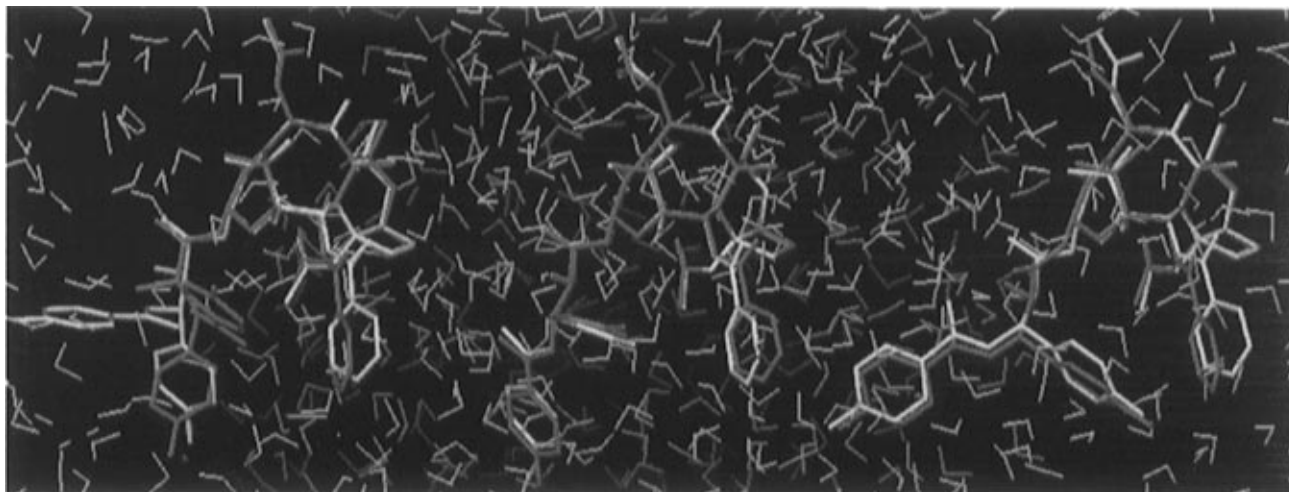

Figure 8. Aqueous RMD study: overlay of starting low-energy structure (magenta) obtained from vacuum RMD study with the lowest energy structure (yellow) obtained in the aqueous simulation for conformers A (left), B (middle), and C (right).

side chain amino acid conformation, supporting its observation in protic media, the observed temperature dependence of $J_{H2'-H3'}$ shown in Figure 4 A indicates a more significant contribution of conformer C at ambient and higher temperatures in DMSO/D_2O and the predominant contribution in CD_3OD/D_2O and CD_3OD at ambient temperature. The slopes for the J values in CD_3OD also indicate a quite likely participation of conformer A at higher temperatures in this solvent since the J value becomes smaller than 5.2 Hz, which corresponds to conformer C. The gap between the RMD energy estimation and the NMR data can be ascribed to the fact that the RMD calculations give the enthalpy of the molecules, but not the total free energy; i.e., the entropy term is not included. Since the order of molecular organization is highest in conformer B and the lowest in conformer A, and conformer C is in between on the basis of the vacuum RMD results shown in Figure 7, the entropy of these three conformers should increase in the order conformer B < conformer C < conformer A. This means that the relative free energy gain of the three conformers is temperature dependent and should increase in the order conformer B < conformer C < conformer A. Accordingly, conformer A and conformer C should become favorable at higher temperatures as compared to conformer B. A combination of the strong solvation effects and the entropy term adjustment may well

offset the destabilization caused by the near-eclipsed arrangements of the side chain amino acid in conformer C.

In order to confirm that conformers A, B, and C thus identified are consistent with the 2D NMR studies of paclitaxel and docetaxel reported from other laboratories,[36] we carried out the $^1H-^1H$ NOESY and ROESY measurements of difluoro paclitaxel **3** and fluoro docetaxel **4** in CD_2Cl_2, CD_3OD, CD_3OD/D_2O, and DMSO-d_6/D_2O. As expected, clear NOEs were indeed observed between the 3'-(4-FC_6H_4) and 2-benzoate (Ph) protons in DMSO-d_6/D_2O. Thus, it appears that the presence of the fluorine atoms at the *para* positions of the phenyl rings does not exhibit any significant conformational change in solution. The $^{19}F-^1H$ heteronuclear NOE measurements were also carried out for **3** and **4** in CD_3OD and DMSO-d_6/D_2O (Figures 9 and 10). Although the $^{19}F-^1H$ NOEs were smaller than their $^1H-^1H$ counterparts, cross-peaks were clearly observed between the fluorine of 3'-(4-FC_6H_4) and the phenyl protons of 2-benzoate in these solvents except for **4** in CD_3OD. The presence of these NOEs is consistent with the hydrophobic clustering conformations, i.e., conformers B and C. *However, it should be noted that these NOEs are very likely to be for an averaged structure of conformers B and C.* No $^1H-^1H$ and $^{19}F-^1H$ NOEs between 3'-(4-FC_6H_4) and 2-benzoate moieties were observed in CD_2Cl_2 or $CDCl_3$ for both com-
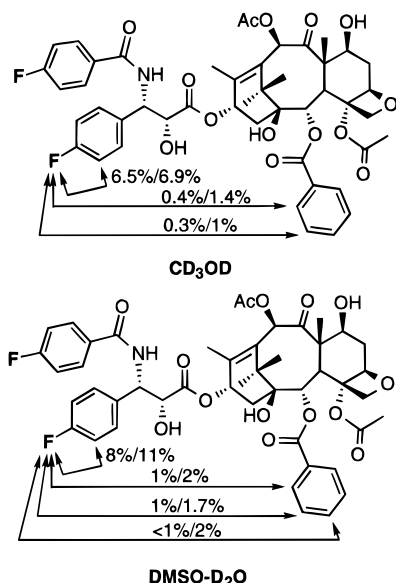
Figure 9. Representative ^{1}H$-^{19}$F heteronuclear NOEs for **3** in CD$_3$OD and DMSO-d_6/D$_2$O at 25 °C.
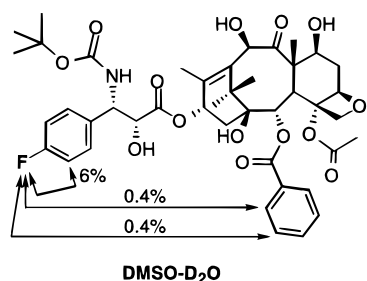
Figure 10. Representative ^{1}H$-^{19}$F heteronuclear NOEs for **4** in DMSO-d_6/D$_2$O at 25 °C.

pounds. Despite the apparent clustering of the two aryl groups of 4-C$_6$H$_4$CONH (or PhCONH for paclitaxel) and 2-benzoate of the energy-minimized conformer A (or structure **A** for paclitaxel), no NOEs have ever been observed between the two groups in this study as well as previous ones. The only NOEs observed in CD$_2$Cl$_2$ for **3** and **4** are those between the *p*-fluorine and the adjacent *meta* protons on the aromatic rings. These results strongly suggest the substantial flexibility of this conformation in solution, which is indeed confirmed by our RMD study of conformer A as discussed above.

The conformational analysis of fluoro docetaxel **4** is more complicated than that of **3**. In CD$_2$Cl$_2$, the *J* values were small (2.0−2.2 Hz) and difficult to measure due to the overlap and broadening of peaks. The clear temperature dependence of the ^{19}F chemical shift in DMSO-d_6/D$_2$O, CD$_3$OD/D$_2$O, and CD$_3$OD as well as the decoalescence of the fluorine of the 4-FC$_6$H$_4$ group at C-3′ in CD$_3$OD at low temperatures is also observed for **4** (Figures 2 and 3). In this case, the ratio of F$_{B-1}$ to F$_{B-2}$ is ca. 2:3 at 198 K although the two peaks are not very well separated (Figure 3). As Figure 4B (bottom) shows, the coupling constant $J_{H2'-H3'}$ is dependent on temperature and the solvent in a manner similar to the case of **3**. However, the value of the coupling constant in each solvent and its variation with temperature for **4** are considerably smaller than those observed for **3**. It should be noted that the extrapolated $J_{H2'-H3'}$ value in DMSO-d_6/D$_2$O at 183 K is only 8.8 Hz; i.e., it does not reach ca. 10 Hz which corresponds to a H2′−C2′−C3′−H3′ torsion angle of 178° (conformer B). As Figure 10 shows, no hetero-NOEs are observed for **4** in CD$_3$OD between the 3′-(4-FC$_6$H$_4$) and 2-benzoate (Ph) protons. These results clearly indicate a substantial contribution of conformer A in all solvents and in a

wide temperature range. Accordingly, it is highly likely that the conformational equilibria for **4** should include all three conformers. This makes the conformational analysis based on the $J_{H2'-H3'}$ values very difficult because of the three-component system. Nevertheless, we can still confirm the predominant contribution of the hydrophobic clustering conformations (conformers B and C) in DMSO-d_6/D$_2$O. This is also supported by the fact that hetero-NOEs are observed between the fluorine of the 3′-(4-FC$_6$H$_4$) group and protons of the 2-benzoate moiety although the intensities are much weaker than those observed for **3**, which again strongly indicates the substantial contribution of conformer A even in DMSO-d_6/D$_2$O. It is very likely that the butoxycarbonyl group in place of the benzoyl group at the C3′−N position increases the flexibility of the molecule. Consequently, we can conclude that the distribution of the conformer population for paclitaxel and docetaxel as a function of solvent and temperature is quite different.

Williams et al. have recently reported an NMR and molecular modeling study on the biologically inactive 2′-acetylpaclitaxel in CDCl$_3$ and aqueous DMSO-d_6 solutions.[49] It was reported that 2′-acetylation had negligible effects on the conformation of this molecule in these solvents, which implies that conformational preorganization of the isoserine side chain is not dependent upon hydrogen bonding using the 2′-OH. It is suggested that the 2′-OH is likely to serve as a hydrogen bond donor that is necessary for effective binding to tubulin/ microtubules. With this in mind we prepared fluoro 2′,10-diacetyldocetaxel **5** (*vide supra*), and looked at its dynamic behavior using ^{19}F VT NMR in the same manner as the cases of **3** and **4**. The ^{19}F VT NMR measurements in MeOH did not show any decoalescence and freeze-out of conformers at temperatures as low as 188 K. It is clear that the acetylation of the 2′-OH group destroys the intramolecular hydrogen-bonding network and increases the mobility of the molecule, hence preventing the decoalescence of the two conformers from occurring even at very low temperatures.

Although the major driving force for the stability of conformers B and C appears to be the hydrophobic clustering among the 3′-Ph, 2-benzoate (Ph), and 4-acetoxy (CH$_3$) moieties, hydrogen bonding in the side chain can also substantially contribute to the stabilization. As Figure 6 shows, there are three hydrogen bonds on the isoserine side chain between the C-1′ ester C(O) and 2′-O(H), C-2′ (O) and 3′-N(H), and 2′-O(H) and 4-FC$_6$H$_4$C(O). When the 2′-OH moiety is acetylated, the hydrogen bondings between the C-1′ ester C(O) and 2′-O(H) as well as 2′-O(H) and 4-FC$_6$H$_4$C(O) are the ones most directly affected. While molecular modeling and NMR analyses (at room temperature) of 2′-acetylpaclitaxel[49] and **5** indicate that there is no significant conformational changes as compared to paclitaxel, the aforementioned ^{19}F VT NMR study clearly indicates that this modification exerts marked effects on the dynamic behavior of the molecule. In CD$_2$Cl$_2$ (or CDCl$_3$), it is obvious that intramolecular hydrogen bondings are responsible for the strong self-organization, which is virtually not affected by temperature.

In conclusion, the fluorine probe approach has been proved to be very useful for the conformational analysis of paclitaxel and taxoids in connection with the determination of possible bioactive conformations. A previously unrecognized conformer C is found to play a significant role in the conformational equilibrium of paclitaxel. This conformation might be the molecular structure first recognized by the β-tubulin binding

(49) Williams, H. J.; Moyna, G.; Scott, A. I.; Swindell, C. S.; Chirlian, L. E.; Heerding, J. M.; Williams, D. K. *J. Med. Chem.* **1996**, *39*, 1555−1559.

site on microtubules. Incontrovertible evidence for the existence of conformer C in different polar media has been obtained on the basis of a variety of techniques including VT NMR, molecular modeling, and restrained molecular dynamics. Further studies along this line are actively underway. The next challenge will be to use a paclitaxel analog with triple fluorine label at all three phenyl groups and determine the distances between these three fluorines for the trifluoro paclitaxel$-\beta$-tubulin complex, probably by solid state NMR.

Experimental Section

Materials. 3'-Dephenyl-3'-(4-fluorophenyl)-3'N-debenzoyl-3'N-(4-fluorobenzoyl)paclitaxel (**3**), 3'-dephenyl-3'-(4-fluorophenyl)docetaxel (**4**), and 10-acetyl-3'-dephenyl-3'-(4-fluorophenyl)docetaxel (**6**) were prepared by using the procedures reported previously from these laboratories.[24] 2',10-Diacetyl-3'-dephenyl-3'-(4-fluorophenyl)docetaxel (**5**) was prepared through acetylation of 10-acetyl-3'-dephenyl-3'-(4-fluorophenyl)docetaxel (**6**) as follows.

2',10-Diacetyl-3'-dephenyl-3'-(4-fluorophenyl)docetaxel (5). To a solution of **6** in 2 mL of CH_2Cl_2 and N,N-diisopropylethylamine (0.01 mL, 0.06 mmol) at 0 °C was added 5 μL (0.06 mmol) of AcCl. The reaction mixture was allowed to warm to room temperature, at which time another 5 μL of AcCl was added. After 20 min, the reaction mixture was purified by chromatography on silica gel (EtOAc:hexanes = 1:2) to afford 20 mg of **5** (71%) as a white film: ^{1}H NMR (250 MHz, CDCl$_3$) δ 1.08 (s, 3 H), 1.20 (s, 3 H), 1.27 (s, 3 H), 1.68 (s, 3 H), 1.80$-$1.82 (m, 1 H), 1.87 (s, 3 H), 2.05 (s, 3 H), 2.08$-$2.11 (m, 2 H), 2.18 (s, 3 H), 2.37 (bs, 3 H), 2.46$-$2.51 (m, 3 H), 3.75 (d, J = 7.2 Hz, 1 H), 4.11 (d, J = 8.4 Hz, 1 H), 4.25 (d, J = 8.4 Hz, 1 H), 4.35$-$4.41 (m, 1 H), 4.91 (d, J = 7.8 Hz, 1 H), 5.26 (d, J = 2.4 Hz, 1 H), 5.28 (d, J = 8.7 Hz, 1 H), 5.37 (d, J = 8.8 Hz, 1 H), 5.62 (d, J = 7.2 Hz, 1 H), 6.19 (m, 1 H), 6.23 (s, 1 H), 7.03 (t, J = 8.4 Hz, 1 H), 7.20$-$7.22 (m, 2 H), 7.44 (t, 2 H), 8.05 (d, 2 H); ^{13}C NMR (63 MHz, CDCl$_3$) δ 9.6, 14.8, 20.4, 20.8, 22.1, 22.6, 26.8, 28.1, 35.4, 43.2, 45.6, 53.5, 58.5, 71.8, 72.2, 74.2, 75.1, 75.6, 79.2, 80.6, 81.1, 84.4, 115.7, 116.0, 128.0, 128.1, 128.7, 129.1, 130.2, 132.7, 133.3, 143.0, 155.0, 164.4, 167.2, 167.9, 169.6, 171.3, 203.8; FAB-HRMS (NBA$-$NaCl) m/z 932.3524 (M$^+$ + Na, $C_{47}H_{56}NO_{16}F$ requires 932.3481).

NMR Measurements. NMR spectra for **3** and **4** were recorded either on a Bruker ARX-400 (^{1}H, 400 MHz; ^{19}F, 376 MHz) or on a Bruker AC-250 (^{1}H, 250 MHz; ^{19}F, 235 MHz) NMR spectrometer. Samples ($\sim$2 mM) were run in CD_2Cl_2, CD_3OD, CD_3OD/D_2O (3:1), and DMSO-d_6/D$_2$O (3:1). Chemical shifts are reported in parts per million relative to TMS and CFCl$_3$ (for ^{19}F) as internal standards. The variable temperature was monitored by a Eurotherm unit provided by Bruker. In the 1D spectra, coupling constants were measured after a Lorenz$-$Gauss transformation and zero-filling of the FID, in order to obtain a resolution of 0.1 Hz/point. The HMQC, HMBC, and COSY spectra were performed on an inverse multinuclear probehead equipped with a Z-gradient coil. The hetero-NOEs were performed on an inverse dual probehead (^{19}F$-^1$H) using a modified version of the original Bruker steady state NOE difference pulse program (noediff or noemult). For each frequency, the overall irradiation time was about 8 s per cycle, with a minimum of 50 cycles. The NOE was quantified with a reference to $\sim$100% measured on the "off resonance" spectrum, the difference spectrum thus giving directly the intensity of the NOE. The ROESY spectra were recorded at 298 K with a relaxation delay of 1.5 s and 512 experiments of 1-K data points, sinebell-shifted by a $\pi/6$

multiplication in both dimensions (sweep width of about 4000 Hz). Three mixing times of 220, 600, and 1000 ms were used.

Molecular Modeling. Computational studies were carried out on a Silicon Graphics Iris 4D/35 workstation. Dihedral (torsion) angle constraints were derived from the $J_{H2'-H3'}$ coupling constants using the Karplus equation as interpreted by Macromodel 4.0. Restrained molecular dynamics calculations were performed using Sybyl 6.04 (Tripos Inc.) as well as Discover 95.0 in the Insight II (MSI-Biosym) platform. The following protocol was used for the Sybyl 6.04 vacuum simulation: A starting structure was generated from atomic coordinates obtained from the paclitaxel crystal structure[35] in the Cambridge Database and modified with appropriate substituents. Charges were calculated for all simulations (Sybyl 6.04) on the basis of the Gasteiger$-$Marsilii method. This structure was energy minimized (Tripos force field) to an rms derivative below 0.01 kcal/mol/Å. The H2'$-$C2'$-$C3'$-$H3' dihedral angle was restrained to 54°, 124°, or 180°, respectively, prior to running the dynamics simulation. The system was equilibrated at 300 K for 5 ps, following which restrained molecular dynamics was performed over a period of 100 ps at 900 K with a time step of 1 fs. Snapshots were taken every 2 ps. From these, 25 structures were randomly selected and minimized using steepest descents followed by conjugate gradients to an rms derivative below 0.01 kcal/mol/Å. The minimized structures were then subjected to restrained molecular dynamics at 300 K for 2 ps, followed by further minimization using steepest descents and conjugate gradients. These final structures were overlapped using the "Superimpose" function in the Insight II platform.

Water-solvated dynamics studies were conducted using the Discover 95.0 program in the Insight II molecular modeling system (Biosym Technologies/Molecular Simulations, Inc.).[45-47] Solvation of the lowest energy structures obtained from the above vacuum simulation was carried out using the "Soak" function. A layer of 9 Å of discrete water molecules ($\sim$480 waters) was added. Standard CVFF force field charges were included in all simulations. Molecular dynamics (CVFF force field) was performed on the entire system over 25 ps at 300 K following a 5 ps equilibration period. One ensemble was archived at every 1 ps interval. The archived ensembles were minimized using conjugate gradients to a maximum derivative of less than 1.0 kcal/mol/Å. The energies (total and intermolecular nonbond energies) for each conformer were averaged over the 25 minimized systems and reported along with the mean standard deviation and median.

Supporting Information Available: Variable temperature ^{1}H and ^{19}F NMR data for **3**, **4**, and **5**, results of ROESY and hetero-NOE in CD_2Cl_2, CD_3OD, CD_3OD/D_2O, and DMSO-d_6/D$_2$O, summary of the different energy components, and statistical data for the aqueous dynamics simulations (13 pages). See any current masthead page for ordering and Internet access instructions.